Speed limits on swimming of fishes and cetaceans

G Iosilevskii and D Weihs

References	**This article cites 16 articles, 1 of which can be accessed free** http://rsif.royalsocietypublishing.org/content/5/20/329.full.html#ref-list-1
Email alerting service	Receive free email alerts when new articles cite this article - sign up in the box at the top right-hand corner of the article or click **here**

To subscribe to *J. R. Soc. Interface* go to: **http://rsif.royalsocietypublishing.org/subscriptions**

Speed limits on swimming of fishes and cetaceans

G. Iosilevskii* and D. Weihs

Faculty of Aerospace Engineering, Technion, Haifa 32000, Israel

Physical limits on swimming speed of lunate tail propelled aquatic animals are proposed. A hydrodynamic analysis, applying experimental data wherever possible, is used to show that small swimmers (roughly less than a metre long) are limited by the available power, while larger swimmers at a few metres below the water surface are limited by cavitation. Depending on the caudal fin cross-section, 10–15 m s^{-1} is shown to be the maximum cavitation-free velocity for all swimmers at a shallow depth.

Keywords: swimming speed; maximal speed limit; cavitation

1. INTRODUCTION

In a curious example of converging evolution, all of the fastest marine swimmers have similar propulsion systems that are based on a narrow crescent caudal fin, better known as the 'lunate tail' (Lighthill 1969). Dolphins, tunas and mackerel sharks are obvious members of this group. Since the pioneering work of Gray (1936), the maximal speed attainable by these swimmers has been repeatedly debated (e.g. Wardle 1975; Wardle & Videler 1980), undoubtedly fuelled by reports of yellowfin tuna and wahoo swimming faster than 20 m s^{-1} (Walters & Fierstein 1964) and anecdotal reports of dolphins overtaking fast vessels. Yet undisturbed measurements of dolphin swimming (Fish & Rohr 1999) have never resulted in speeds in excess of 15 m s^{-1}, suggesting that reports of much higher speeds could have been biased by proximity to the observing vessel (Weihs 2004).

In this study, we show that a swimming speed in excess of 15 m s^{-1} is hardly possible at a shallow depth due to cavitation of the caudal fin. To this end, we examine possible limits on the maximal speed attainable by lunate tail propulsion, which result from (i) maximal power that can be produced by the swimmer's muscles, (ii) a combination of the hydrodynamic stall of the fin and the (physiological) limit on the maximal tail beat frequency, and (iii) from an onset of cavitation.

Stall, and the associated loss of hydrodynamic lift and rise of drag, is caused by boundary layer separation from the foil surface (Batchelor 1990). The boundary layer separates either due to an unfavourable pressure gradient over the leeward surface of the fin (henceforth referred as 'standard' stall) or due to appearance of vapour bubbles, forming whenever the surface pressure drops below the vapour pressure of the liquid in which the fin moves. The latter phenomenon is known as cavitation (Batchelor 1990). These vapour bubbles move downstream into the area of higher pressure and collapse. If the collapse occurs at the fin surface (and it depends on operating conditions), damage may occur to

the fin surface. If the collapse occurs downstream of the trailing edge, it suggests a cavitation-triggered stall. The unfavourable pressure gradient increases with the increasing angle of incidence of the fin. The surface pressure drops both with the increasing angle of incidence and the swimming speed. Since a high angle of incidence is necessary to increase the speed for a given tail beat frequency, both stall and cavitation limit the thrust produced by the fin and hence set limits on the maximal swimming speed.

Prerequisites to our analysis of the speed limits are relations between the angle of incidence of the fin (or, rather, its lift coefficient), its velocity relative to the fluid, the swimming velocity and, of course, the power required to move the fin. In principle, these relations can be extracted from any of the numerous studies published during the last 40 years; the works of Lighthill (1970), Chopra (1974, 1976), Chopra & Kambe (1977) and Cheng & Murillo (1984) are pertinent examples. Nonetheless, we prefer using none of them 'as is'. Being aimed at calculating the propulsion efficiency and the tail feathering as accurately as possible, they are too detailed for the basic analysis we perform here. Hence, we begin this study by recapitulating the analysis of lunate tail propulsion using as simple an approach as we believe practical.

2. ANALYSIS

2.1. Balance of forces

Consider a fish of length l moving with a constant velocity u in a fluid of density ρ by caudal fin propulsion. The caudal fin has an area S_c; it oscillates laterally with an amplitude $h = \bar{h}l$ and a frequency f, moving with a lateral velocity v. The lift L and drag D of the caudal fin can be expressed in terms of its respective lift and drag coefficients, C_L and C_D,

$$L = \frac{1}{2}\rho(u^2 + v^2)S_c C_L \quad \text{and} \quad D = \frac{1}{2}\rho(u^2 + v^2)S_c C_D. \tag{2.1}$$

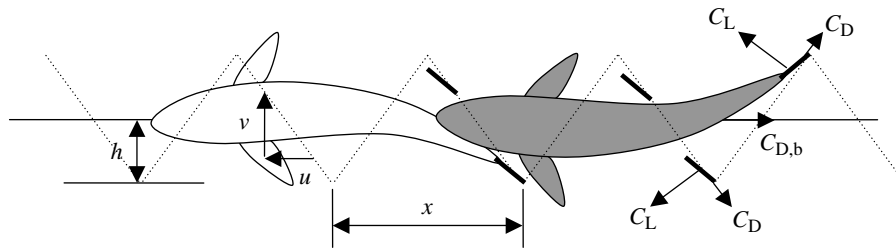*Author for correspondence (igil@aerodyne.technion.ac.il).

Figure 1. Swimming model. With fish body moving along the solid horizontal line, the tail is assumed to move along the dotted sawtooth trajectory. Its wave-length, x, is the stride length and its depth is $2h$. The ratio of $4h$ and x is also the ratio of the (presumably constant) lateral tail velocity v to the (constant) swimming velocity u.

Likewise, the drag of the body, without the fin, can be expressed in terms of its drag coefficient, $C_{D,b}$, by

$$D_b = \frac{1}{2}\rho u^2 S_c C_{D,b}. \tag{2.2}$$

Note that all hydrodynamic coefficients defined thus far, lift and drag of the caudal fin and the drag of the body, use the caudal fin area as the reference area.

In order to simplify the following derivations, it will be assumed that the lateral velocity, v, as well as the lift and drag coefficients, C_L and C_D, of the caudal fin are constants, with v and C_L changing side each half period (figure 1). Limitations of this assumption will be discussed later on.

Now, let $\bar{v} = v/u$ be the ratio of lateral-to-forward velocities. Under the present assumptions, this ratio is closely related with the stride length $\bar{x} = u/fl$—the distance in body lengths travelled during one period. In fact, under present assumptions, $v = 4hf$ and, therefore,

$$\bar{v} = 4\bar{h}/\bar{x}. \tag{2.3}$$

For constant speed swimming, the forward thrust produced by the caudal fin should balance the drag of the fish and the fin combined. Hence, after rearrangement

$$\frac{1}{2}\rho(v^2 + u^2)S_c\left(\frac{vC_L}{\sqrt{v^2+u^2}} - \frac{uC_D}{\sqrt{v^2+u^2}}\right) = \frac{1}{2}\rho u^2 S_c C_{D,b} \tag{2.4}$$

or, eventually,

$$(C_L\bar{v} - C_D)\sqrt{1 + \bar{v}^2} = C_{D,b}. \tag{2.5}$$

2.2. Power

The power spent by the caudal fin during the stroke is given by

$$P = \frac{1}{2}\rho(v^2 + u^2)vS_c\left(\frac{C_L u}{\sqrt{v^2+u^2}} + \frac{C_D v}{\sqrt{v^2+u^2}}\right)$$
$$= \frac{1}{2}\rho u^3 S_c(C_L + \bar{v}C_D)\bar{v}\sqrt{1 + \bar{v}^2}. \tag{2.6}$$

Applying the longitudinal force balance (2.5), equation (2.6) can be recast as

$$P = P_b\left(1 + (1 + \bar{v}^2)^{3/2}\frac{C_D}{C_{D,b}}\right), \tag{2.7}$$

where

$$P_b = \frac{1}{2}\rho u^3 S_c C_{D,b}, \tag{2.8}$$

is the power required to move the fish body (caudal fin excluded) at velocity u, and the term in parentheses can be interpreted as the reciprocal of a propulsive efficiency η, i.e.

$$\eta = \frac{P_b}{P} = \frac{C_{D,b}}{C_{D,b} + (1 + \bar{v}^2)^{3/2}C_D}. \tag{2.9}$$

2.3. Drag coefficients

In order to make use of the above results, the actual values for the drag coefficients are needed. The value of coasting (stretched straight) $C_{D,b}$ for scombrids can be estimated from the data presented in tables V, VI, VII, X and XI of Magnuson (1978); it turns out to be approximately 0.2.[1] The value of $C_{D,b}$ for delphinids and lamnids should be slightly higher owing to the drag of their fixed dorsal and pectoral fins. When strenuously swimming, the average body drag may increase (Fish & Rohr 1999; Weihs 2004). We shall avoid addressing this issue specifically by providing estimates of swimming velocity limits for different drag coefficients.

The drag coefficient of the caudal fin C_D can be estimated based on the standard parabolic relation (Nicolai 1984),

$$C_D = C_{D,0} + kC_L^2, \tag{2.10}$$

where $C_{D,0}$ and k are constants. $C_{D,0}$ is estimated to be approximately 0.01 and is known to be rather insensitive to the particular fin 'design' (Jacobs 1931b); k depends mainly on the fin aspect ratio (Nicolai 1984) and is bounded between 0.05 and 0.1 for all the swimmers mentioned earlier.[2]

---

[1] Based on table V, the body drag coefficient is estimated to be approximately 0.005 when referred to the body surface area. Assuming similarity in body shape among the scombrids (table VII), their surface area can be approximated as $0.45l^2$ (indeed, a 44 cm long skipjack tuna has a surface area of 840 cm^2 (table VI), whereas 40 cm long Kawakawa has the surface area of 720 cm^2 (table XI). At the same time, caudal fin area, for most scombrids, is approximately $0.011l^2$ (table X). Hence, the representative value of $C_{D,b}$ is approximately 0.2—0.005 times the body area divided by the caudal fin area.

[2] For symmetrical cross-sections at the pertinent range of Reynolds numbers, $C_{D,0}$ is typically found between 0.008 and 0.012 (Jacobs 1931b). The value of k can be estimated using semi-empirical formula $k = 1/(\pi Ae) + \delta$, relating it with the aspect ratio A of the fin, span-wise loading correction constant e, typically approximately 0.9, and profile parasite drag rise constant δ, typically approximately 0.01 (Jacobs 1931b; Nicolai 1984). Since $4 < A < 8$ for most scombrids (Magnuson 1978), therefore $0.05 < k < 0.1$.

2.4. Stall and maximal lift coefficient

Any foil can keep the flow attached to both its surfaces only up to a certain angle of attack. Above that angle, the flow on the leeward (suction) surface of the foil separates due to an unfavourable pressure gradient (with pressure increasing towards the trailing edge), causing a loss of lift and an increase in drag; this phenomenon is called 'stall'. At high Reynolds numbers in air, the lift coefficient obtained on the verge of stall is the maximal lift coefficient, $C_{L,max}$, which can be generated by the foil. It varies between 1.0 and 1.2 (Jacobs 1931a,b) for both scombrids, which have a relatively thin caudal fin cross-section with a thickness-to-chord ratio of approximately 0.09 (F. Fish 2006, personal communication), and delphinids and lamnids, which have a much thicker caudal cross-section with thickness-to-chord ratio of up to 0.2 (Lingham-Soliar 2005).

2.5. Cavitation

At sufficiently high swimming velocity, the pressure due to acceleration of the flow around the leading edge may locally drop below the vapour pressure, causing vapour-filled cavities (bubbles) to appear. This phenomenon is known as cavitation (Batchelor 1990). The bubbles are carried downstream by the flow into the rear high-pressure region mentioned above, where they collapse. If the collapse occurs on the surface of the foil, it can damage the surface of the foil. If the collapse occurs downstream of the training edge, it suggests a fully separated flow regime, which can be referred to as a cavitation-induced stall. In apparent contrast with the standard pressure-gradient-induced stall, the lift coefficient obtained on the verge of cavitation-induced stall is not necessarily the maximal possible lift coefficient at that velocity. This maximal (cavitating) lift coefficient is probably almost the same as the non-cavitating $C_{L,max}$. The main difference between the two is in the associated drag coefficient, which is an order of magnitude larger in the cavitating flow.

The lift coefficient $C_{L,c}$ at which cavitation appears is derived in appendix A. It is given, approximately, by

$$C_{L,c} \approx \tau \sqrt{\frac{u_d^2}{u^2(1+\bar{v}^2)} - 1}, \qquad (2.11)$$

where τ is a parameter depending on the foil section and u_d is a parameter depending both on the foil section and on the fluid pressure at the swimming depth. For example, for a Joukowski profile (Milne-Thomson 1973) of thickness t and chord c moving at depth d,

$$\tau = \pi\sigma\sqrt{24\sigma}, \qquad (2.12)$$

$$u_d = \sqrt{\frac{p_0 + \rho g d}{3\sigma\rho}}, \qquad (2.13)$$

where

$$\sigma = \frac{4}{\sqrt{27}}\frac{t}{c} \qquad (2.14)$$

is the shape parameter; p_0 is the atmospheric pressure; and g is the acceleration owing to gravity. For different cross-section shapes, the expression for $C_{L,c}$ has a similar form, but with a slightly different relation between σ and the thickness ratio t/c. Typical values of τ range from 0.28 to 0.93—the former is the characteristic of the 8–9% chord thick sections of scombrids (F. Fish 2006, personal communication), and the latter is the characteristic of the 20% chord thick sections of delphinids and lamnids (Lingham-Soliar 2005). Associated values of u_d, when swimming near the sea surface, range between 22 and 15 m s^{-1}, respectively.

Equation (2.11) indicates that cavitation will precede the standard stall whenever the fin velocity $u\sqrt{1+\bar{v}^2}$ exceeds $u_d\tau/\sqrt{C_{L,max}^2 + \tau^2}$, i.e. approximately 6 m s^{-1} for scombrids and 10 m s^{-1} for delphinids and lamnids near the sea surface. Cavitation becomes imminent at any lift coefficient once the fin velocity exceeds u_d. However, since the fin velocity is always greater than the swimming velocity and swimming requires a finite (non-zero) lift coefficient to produce thrust, the swimming velocity at which cavitation develops will always be lower than u_d, as, indeed, will be shown below.

3. SWIMMING VELOCITY LIMITS

3.1. Power limit

Given any swimming velocity u, there are an infinite number of combinations of the lift coefficient and the lateral velocity satisfying equation (2.5). For each combination, the power required to move the fish through water can be computed using equation (2.7). The power is infinite for both vanishingly small and infinitely large lift coefficients—$\bar{v}$ turns infinite for the former by equation (2.5), and C_D turns infinite for the latter by equation (2.10). Hence, the power has a minimum $P_{min} = P_b/\eta_{max}$ for a certain finite lift coefficient (at which the propulsion efficiency η reaches its maximum η_{max}). At the same time, there exists a (physiological) maximum P_{max} on the available power in the fish muscles. Combination of (hydrodynamic) P_{min} and (physiological) P_{max} yields a limit

$$u_{max,P} = \sqrt[3]{\frac{2\eta_{max}P_{max}}{\rho S_c C_{D,b}}}, \qquad (3.1)$$

on the maximal swimming velocity.

Lift coefficient C_L^+ yielding a minimum of P (or, equivalently, a maximum of the propulsion efficiency η) can be found by differentiating equation (3.1), subject to equation (2.5), with respect to C_L and equating the result to zero. With details found in appendix B, the result is shown in figure 2. Here, $E^* = 1/(2\sqrt{C_{D,0}k})$ and $C_L^* = \sqrt{C_{D,0}/k}$ are the best hydrodynamic efficiency (lift-to-drag ratio) of the caudal fin and the lift coefficient at which this efficiency is achieved. Typical values of the optimal lift coefficient for all swimmers addressed herein vary between 0.25 (low aspect fins) and 0.3 (high aspect fins) with corresponding efficiencies of 0.86–0.89. These values are on the higher side, since they exclude unsteady effects (Lighthill 1970).
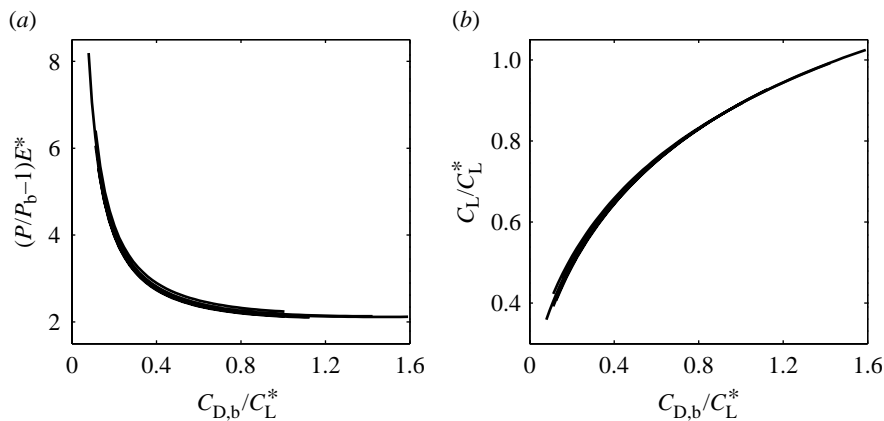
Figure 2. Minimal power required for (*a*) swimming and (*b*) the associated lift coefficient. $C_{D,0}$ varies between 0.008 and 0.02 (about twice its maximal expected value), and k varies between 0.05 and 0.1. (*a*,*b*) All feasible combinations of these parameters result in practically indistinguishable differences.

The maximal available power can be always expressed as a product

$$P_{\max} = \rho_b V_b \bar{P}_{\max}, \qquad (3.2)$$

of the maximal available power per unit mass of the swimmer, $\bar{P}_{\max}$, and the swimmer's mass, $\rho_b V_b$; ρ_b and V_b being the body density and volume, respectively. The body volume for scombrids can be estimated from the data collected by Magnuson (1978); based on his table VII and a typical body shape found in his fig. 10, V_b is approximately $0.02l^3$ for *Thunnus*, *Euthynnus* and *Auxis*, and approximately $0.01l^3$ for *Scomber*. The body density can be found in his table III, but for the sake of simplicity it can be set roughly equal to that of water.

We could not find a consensus value in the literature for the maximal available power per unit mass, $\bar{P}_{\max}$. It is obviously species and conditions dependent, increasing with body temperature. In the following discussion, we have bracketed $\bar{P}_{\max}$ with values ranging from 10 to $160 \, W \, kg^{-1}$ (Azuma 1992). The resulting values of $u_{\max,P}$ are shown in figure 6 at the end of this paper. In the interim, we note that since caudal fin area changes, approximately, with the length of the swimmer squared, whereas the maximal available power varies, approximately, with the length of the swimmer to the third power, equation (3.1) shows that the maximal velocity due the available power limit increases with cube root of the swimmer's length. Hence, insofar as this limit is concerned, the fastest swimmers should have large-volume (high $P_{\max}$) streamlined bodies (low $S_c C_{D,b}$) and high aspect ratio tails (high $\eta_{\max}$). They should preferably have high body temperature (high $\bar{P}_{\max}$). Indeed, all are distinctive features of delphinids, scombrids and lamnids.

3.2. Cavitation limit

Substituting equations (2.10) and (2.11) into equation (2.5) results in the equation

$$\bar{v}\tau\sqrt{\frac{u_d^2}{u^2} - 1 - \bar{v}^2} - \frac{1}{\sqrt{1 + \bar{v}^2}}$$

$$\times \left(C_{D,0}(1 + \bar{v}^2) + k\tau^2\left(\frac{u_d^2}{u^2} - 1 - \bar{v}^2\right) \right) = C_{D,b},$$

$$(3.3)$$

for the reduced lateral tail velocity $\bar{v}$ (or its reciprocal, which is proportional to the stride length) enabling swimming at velocity u with caudal fin on the verge of cavitation. Conversely, it can be solved to obtain the cavitation incipient swimming velocity at a given stride length

$$\frac{u}{u_d} = \frac{k\tau}{\sqrt{1 + \bar{v}^2}}\left(\frac{\bar{v}^2}{2} - k\frac{C_{D,b} + C_{D,0}\sqrt{1 + \bar{v}^2}}{\sqrt{1 + \bar{v}^2}} \right.$$

$$\left. + k^2\tau^2 \pm \frac{\bar{v}^2}{2}\sqrt{1 - \frac{4k}{\bar{v}^2}\frac{C_{D,b} + C_{D,0}\sqrt{1 + \bar{v}^2}}{\sqrt{1 + \bar{v}^2}}} \right)^{-(1/2)}.$$

$$(3.4)$$

The solution of equation (3.3) is shown in figure 3. First, it is apparent that above a certain velocity (henceforth referred as 'u_c'), swimming cannot be sustained without cavitation. Below that threshold, equation (3.3) has two solutions, $\bar{v}_{c,1}$ and $\bar{v}_{c,2}$. Cavitation can be avoided only if $\bar{v}$ is kept between the two—moving the tail slower requires higher lift coefficient and hence invokes cavitation, and moving the tail faster increases the apparent flow velocity and invokes cavitation as well.

The solutions of equation (3.3) for a given u have no closed analytical form in the general case. Yet

$$u_c \approx \frac{u_d}{\sqrt{1 + 2\frac{C_{D,b} + C_{D,0}}{\tau}}} \qquad (3.5)$$

$$\bar{v}_c = \bar{v}_{c,1} = \bar{v}_{c,2} \approx \sqrt{\frac{C_{D,b} + C_{D,0}}{\tau}} \qquad (3.6)$$

and

$$C_{L,c} \approx \tau\sqrt{\frac{C_{D,b} + C_{D,0}}{\tau + C_{D,b} + C_{D,0}}} \qquad (3.7)$$

provide good approximations for the maximal swimming velocity, the corresponding stride length $\bar{x}_c = 4\bar{h}/\bar{v}_c$ and the associated lift coefficient (figures 3 and 4).
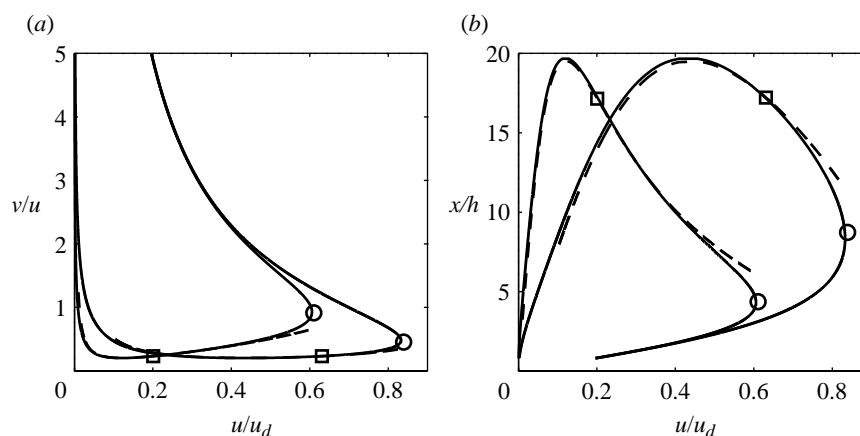
Figure 3. Estimated cavitation-free envelopes on (*a*) the lateral tail velocity and (*b*) the stride length; cavitation is avoided inside the envelopes. Right extending envelopes correspond to a typical dolphin-like swimmer with 0.2 chord thick fin having $C_{D,b}/\tau = 0.2$, $C_{D,0}/\tau = 0.01$ and $\tau k = 0.05$; inner envelopes correspond to a typical tuna-like swimmer with 0.09 chord thick fin having $C_{D,b}/\tau = 0.8$, $C_{D,b}/\tau = 0.04$ and $\tau k = 0.0125$. Broken lines mark the approximation (3.8), circles mark the maximal speed estimate of equations (3.5) and (3.6) and squares mark cavitation appearing at $C_{L,1} = 1.2$.
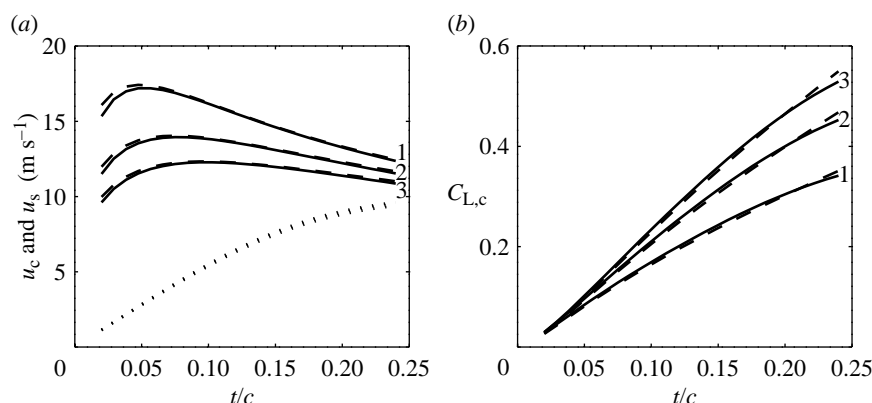

Figure 4. Maximal swimming velocity possible with (*a*) no cavitation near the sea surface and (*b*) the caudal fin lift coefficient at that velocity, plotted against caudal fin thickness-to-chord ratio. Solid lines mark exact numerical solution for the maximum of equation (3.4) and broken lines mark the estimate based on equations (3.5) and (3.7). (*a*) The dotted line marks the maximal swimming velocity possible with no cavitation when the fin is at $C_L = 1.2$. $C_{D,b}$ equals 0.1 (line 1), 0.2 (line 2) and 0.3 (line 3); $C_{D,0} = 0.01$ and k changes between 0.05 and 0.1 (the difference is imperceptible in the figure).

Likewise,

$$\bar{v}_{c,1} \approx \frac{C_{D,b} + C_{D,0}}{\tau} \frac{1}{\sqrt{\frac{u_d^2}{u^2} - 1}} + \tau k \sqrt{\frac{u_d^2}{u^2} - 1} \qquad (3.8)$$

and

$$C_{L,1} \approx \tau \sqrt{\frac{\left(\frac{u_d^2}{u^2} - 1\right)^2 - \left(\frac{C_{D,b} + C_{D,0}}{\tau}\right)^2}{\left(\frac{u_d^2}{u^2} - 1\right) + \left(\frac{C_{D,b} + C_{D,0}}{\tau}\right)^2}} \qquad (3.9)$$

provide good approximations for the minimal lateral velocity (maximal stride length) and the corresponding lift coefficient at no-cavitation boundary (figures 3 and 4).

It was mentioned earlier (see paragraph following equation (2.14)) that cavitation will precede the standard stall only if the fin velocity $u\sqrt{1 + \bar{v}^2}$ is larger than $u_d \tau / \sqrt{C_{L,max}^2 + \tau^2}$. Equation (3.9) allows finding the corresponding swimming velocity u_s. In fact, setting $C_{L,1} = C_{L,max}$ therein and solving it for u/u_d yields an

estimate,

$$u_s \approx u_d \left(1 + \frac{C_{L,max}^2}{2\tau^2} + \frac{1}{2\tau^2} \right.$$
$$\left. \sqrt{C_{L,max}^4 + 4(C_{D,b} + C_{D,0})^2 \left(\tau^2 + C_{L,max}^2 \right)} \right)^{-(1/2)},$$

$$(3.10)$$

for the maximal swimming velocity possible with no cavitation when the fin is on the verge of stall.

The maximal possible swimming velocity with no cavitation, u_c is shown in figure 4 for representative values of the body drag coefficients; it is somewhere between 10 and 15 m s^{-1}. This velocity is insensitive to the fin planform (indeed, approximation (3.5) for u_c is independent of k); it increases as the fin area increases (lower $C_{D,b}$) and it has a maximum for thickness-to-chord ratio of 0.06–0.1. Perhaps a coincidence, but these values are characteristic for scombrids.

The maximal swimming velocity with no cavitation at $C_{L,max}$, u_s, is also shown in figure 4. It almost equals u_c for delphinids and lamnids (having a thickness ratio of
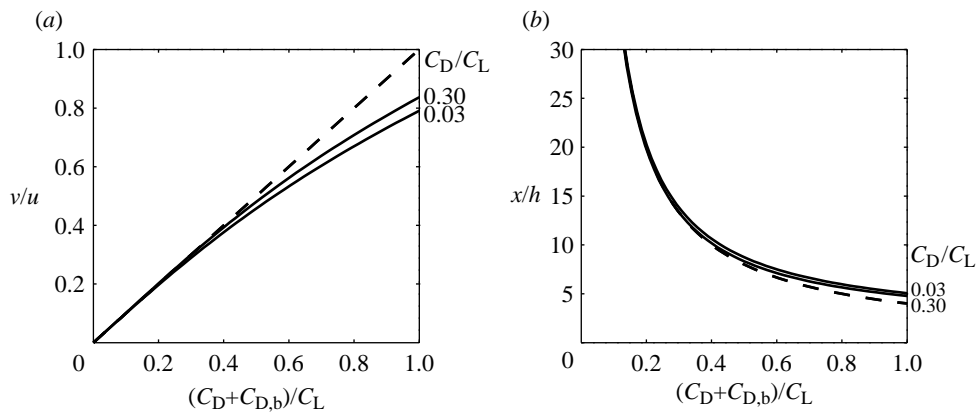
Figure 5. (*a*) Minimal lateral tail velocity and (*b*) maximal stride length. Broken lines mark approximation (3.11). The values of C_D/C_L in the figure range between 0.03 and 0.3; they are marked to the right of the respective lines.

0.2), but it is less than half of u_c for scombrids. In other words, delphinids can swim on the verge of stall increasing speed by increasing the tail beat frequency up until cavitation appears. There remains very little to gain in the maximal speed by reducing the lift coefficient and increasing the beat frequency. Scombrids can accelerate on the verge of stall only up to a relatively small velocity—almost one-third of their maximal cavitation-free velocity. The latter can be reached only by significantly reducing the lift coefficient. It can be achieved only through excessive (when compared with delphinids) flexibility of the tail joint.

3.3. Maximal tail beat frequency limit

Given the lift coefficient of the fin, C_L, equation (2.5), subject to equation (2.10), can be solved to yield the reduced lateral velocity of the tail, $\bar{v}$, required to sustain swimming velocity at that lift coefficient. Although this solution cannot be expressed in a closed analytical form in the general case, for all practical values of lift and drag coefficients,

$$\bar{v} \approx \frac{(C_{D,b} + C_D)}{C_L}, \tag{3.11}$$

provides a very good approximation (figure 5a). The associated stride length, $\bar{x} = 4\bar{h}/\bar{v}$, is shown in figure 5b.

At the same time, there exists a (physiological) maximum f_{max} on the possible tail beat frequency, and hence there exists a constraint $v_{max} = 4\bar{h}lf_{max}$ on the maximum possible lateral tail velocity. Combining the (hydrodynamic) requirement of $\bar{v}$ and (physiological) limit v_{max} of v yields a limit

$$u_{max,f} = \frac{v_{max}}{\bar{v}} = \frac{4\bar{h}lf_{max}}{\bar{v}}, \tag{3.12}$$

on the maximal swimming velocity at C_L. Obviously, a prerequisite of reaching the cavitation limit addressed in §3.2 is the ability of the swimmer to move its tail fast enough. Formally, it is required that v_{max} should exceed $\bar{v}_{c,1}u$.

Equation (3.11) implies that $\bar{v}$ tends to infinity as C_L tends to either zero or infinity. Hence, $\bar{v}$ has a minimum

$\bar{v}_{min}$; it is shown in appendix C that, in the non-cavitating flow regime, this minimum is obtained at the highest possible value of the lift coefficient, i.e. at $C_{L,max}$ or $C_{L,1}$, whichever is smaller.

We could not find a consensus value in the literature for the maximal beat frequency; hence, we shall avoid substituting any numbers. The trends however are of interest. Assuming for a moment that a fish consists of an elastic material having an effective Young modulus E_b (e.g. Collinsworth *et al.* 2002) and density ρ_b, let $a = \sqrt{E_b/\rho_b}$ be the longitudinal wave propagation velocity (e.g. Graff 1975). Response time of an elastic body to an impulse should be proportional to the ratio of the characteristic length to the propagation velocity, i.e. the ratio l/a.

The contraction of a muscle is triggered by Ca^{++} ion concentration (Johnston 1983; Vander *et al.* 1985). Hence, there is a time delay between the arrival of the nerve signal (action potential) and the beginning of the muscle motion. Combining the (physiological) time delay with the (elastic) response time suggests that the maximal beat frequency can be approximated by the ratio

$$f_{max} \propto \frac{a}{l + l_0}, \tag{3.13}$$

where l_0 is a certain constant associated with the time delay.

A 'real' muscle is composed of cells that are approximately of the same size for small and large fishes alike. Hence, the propagation velocity (directly dependent on the cells-averaged value of the effective Young modulus) should be insensitive to the body length. At the same time, both Ca^{++} ion concentration and the propagation velocity are governed by a series of enzymatic reactions (Vander *et al.* 1985). The reaction rates increase with temperature, increasing a and decreasing l_0, and hence increasing f_{max}.

Combining equation (3.13) with equation (3.12), it appears that, insofar as the maximal beat frequency limit on the swimming velocity is concerned, the fastest swimmers should be large and warm bodied. Yet, for very large swimmers (for which propagation time is large when compared with the time delay) the maximal beat frequency limit on the swimming
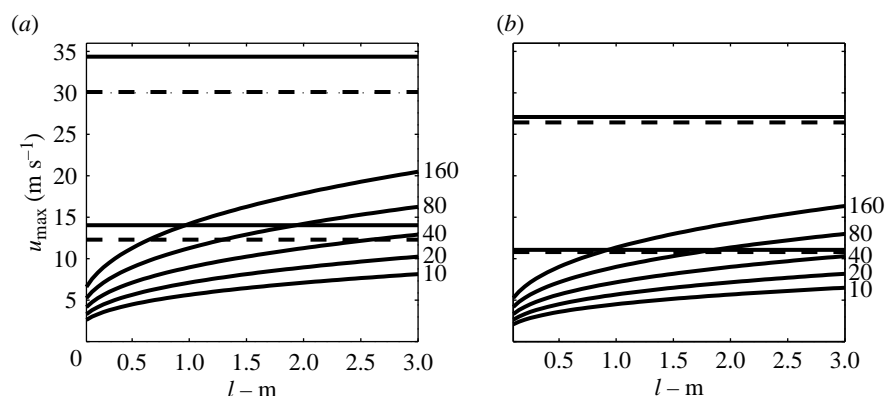
Figure 6. Maximal swimming velocity with $\bar{h}=0.2$, $C_{D,0}=0.01$, $k=0.05$, $C_{L,max}=1.2$, (a) $C_{D,b}=0.2$ and (b) $C_{D,b}=0.4$. Curved solid lines mark power limit on the swimming velocity—the respective power per unit mass of the fish is marked to the right of each line. The horizontal lines mark cavitation limits for 9% (solid lines) and 20% (dashed lines) thick foils near the surface (lower sets) and at the depth of 50 m (higher sets).

velocity (whether associated with the onset of cavitation or with the onset of stall) turns out to be independent of the body length.

4. DISCUSSION

Power and cavitation limits on the swimming velocity have been combined in figure 6. Maximum tail beat frequency limit has not been shown owing to the uncertainty in the particular value of that frequency.

Since the maximal power-limited velocity increases, roughly, with the cube root of the body length, and since both cavitation and tail beat frequency limits (for large fishes) are independent of the body length, all fishes are power limited when small and either cavitation or tail beat frequency limited when large. The particular body length at which the available power limit is no longer the most severe constraint is conditions (body temperature and depth) dependent. Large swimmers at depth may have their top speed limited by the combination of the standard stall of the caudal fin and the maximal tail beat frequency; large swimmers near the water surface may have their top speed limited by cavitation.

In fact, cavitation poses a real limit on warm-bodied large swimmers at shallow depth, with 10–15 m s^{-1} being the maximal cavitation-free velocity. Above that speed cavitation is imminent. Lacking pain receptors on their caudal fins, scombrids may temporarily cross the cavitation limit, and cavitation-induced damage has been observed (Kishinouye 1923); on the other hand, delphinids probably cannot cross it without pain (Lang 1966).

We have tacitly avoided unsteady hydrodynamic effects and assumed that the caudal fin alignment—and possibly flex—is adjusted so as to provide constant lift coefficient during the beat cycle. For a given lift coefficient, chord-wise flexibility (Katz & Weihs 1978) will increase the leading edge suction causing cavitation at lower swimming speeds. Unsteady effects will increase the drag coefficient of the tail, but since its drag is normally small when compared with that of the fish body, it will only have a small effect on the velocity limits as discussed above.

APPENDIX A. CAVITATION LIMIT ON THE LIFT COEFFICIENT OF HYDROFOILS

Consider an aerofoil generated by Joukowski transformation (Milne-Thomson 1973)

$$\zeta = z + \frac{a^2}{z}, \qquad (A\,1)$$

of a circle

$$z = a(\sigma + (1+\sigma)e^{i\theta}), \qquad (A\,2)$$

$\theta \in [-\pi,\,\pi)$ on the complex plane. It is a symmetrical aerofoil of chord

$$c = 4a(1 + O(\sigma^2)), \qquad (A\,3)$$

thickness

$$t = c\frac{3\sqrt{3}}{4}\sigma(1 + O(\sigma^2)) \qquad (A\,4)$$

and leading edge radius

$$r_{LE} = 2c\sigma^2. \qquad (A\,5)$$

Its leading edge is generated by the part of the circle near the real axis on the right-half plane, i.e. where θ is small.

The complex potential W about this aerofoil, which satisfies the Kutta condition at its trailing edge is

$$W(z) = -u_\infty e^{i\alpha}(z-a\sigma) - u_\infty e^{-i\alpha}\frac{a^2(1+\sigma^2)^2}{(z-a\sigma)}$$

$$-2iu_\infty a(1+\sigma)\sin\alpha\ln(z-a\sigma), \qquad (A\,6)$$

where u_∞ is the velocity of the flow (from right to left) and α is the angle of attack, i.e. the angle between the oncoming flow and the chord. The velocity Q on the surface of this aerofoil immediately follows equation (A 6) by definition of the complex potential (Batchelor 1990); it yields

$$Q(\theta) = \lim_{z\to a(\sigma+(1+\sigma)e^{i\theta})} \left(\frac{dW(z)}{dz}\frac{dz}{d\zeta}\right)$$

$$= -u_\infty\frac{2ie^{-i\theta}(\sigma+(1+\sigma)e^{i\theta})^2}{(\sigma+(1+\sigma)e^{i\theta})^2-1}(\sin(\alpha+\theta)+\sin\alpha).$$

$$(A\,7)$$

The pressure p and the associated pressure coefficient,

$$C_P(\theta) = 2\frac{p(\theta)-p_d}{\rho u_\infty^2}, \qquad (A\,8)$$

on the aerofoil surface immediately follow Bernoulli's theorem,

$$p(\theta) = p_{\mathrm{d}} + \frac{1}{2}\rho u_\infty^2 - \frac{1}{2}\rho |Q(\theta)|^2, \qquad (A\ 9)$$

where p_{d} is the pressure of the unperturbed fluid.

Now consider a particular thin Joukowski aerofoil at a small, but non-zero angle of attack. Formally, we set $\alpha = \bar{\alpha}\varepsilon$ and $\sigma = \bar{\sigma}\varepsilon$ where ε is a certain small parameter and all marked quantities are of the order of unity. For the analysis of the cavitation limit on aerofoil performance, we seek the lowest pressure developing on the aerofoil surface. It is assumed—subject, of course, to an *a posteriori* verification—that the lowest pressure develops in the vicinity of the leading edge, i.e. where $\theta = \bar{\theta}\varepsilon$. Thus,

$$Q(\theta) = -\mathrm{i}u\left(\frac{2\alpha + \theta}{2\sigma + \mathrm{i}\theta}(1 + 3\sigma) + O(\varepsilon^2)\right). \qquad (A\ 10)$$

From equations (A 8)–(A 10), it immediately follows that:

$$c_{\mathrm{P}}(\theta) = 1 - \frac{(2\alpha + \theta)^2}{4\sigma^2 + \theta^2}(1 + 6\sigma) + O(\varepsilon^2). \qquad (A\ 11)$$

This function has a minimum

$$c_{\mathrm{P,min}} = -\frac{\alpha^2}{\sigma^2}(1 + 6\sigma) - 6\sigma + O(\varepsilon^2), \qquad (A\ 12)$$

at

$$\theta_{\min} = \frac{2\sigma^2}{\alpha + O(\varepsilon^2)}. \qquad (A\ 13)$$

Since $\sigma^2/\alpha = \varepsilon\bar{\sigma}^2/\bar{\alpha}$ by definition, and all marked quantities were assumed to be of the order of unity, equation (A 13) confirms our initial assumption that $\theta_{\min}$ is small. In fact, for an infinitely thin section, the minimal pressure is exactly at the leading edge (Milne-Thomson 1973). However, equation (A 12) should be applied with caution for a thick section at a very small angle of attack, where the point of minimal pressure moves away from the leading edge towards the thickest part of the section and $\theta_{\min}$ may no longer be assumed small.

In spite of being approximate and based on a thin Joukowski section, the estimate of (A 12) for the minimal pressure developing on an aerofoil nicely fits the results reported by Lang (1966) for a thick, 0.2 chord, dolphin caudal fin section (figure 7).

Based on general physical considerations, the minimal pressure developing on a wing section is a local phenomenon depending on the lift of the section (which defines the circulation about the section) and a local curvature. We therefore suggest, without a derivation, that the variant

$$C_{\mathrm{P,min}} = -\alpha^2 \frac{2c}{r_{\mathrm{LE}}}\left(1 + 6\sqrt{\frac{r_{\mathrm{LE}}}{2c}}\right) - 6\sqrt{\frac{r_{\mathrm{LE}}}{2c}} + O(\varepsilon^2)$$
$$(A\ 14)$$

of equation (A 12), where all σs have been replaced using equation (A 5), may have a wider application than equation (A 12). In fact, using equation (A 14) with the value of the leading edge radius measured by Lang (1966) offers a better fit to his data than equation (A 12) with the measured value of the section thickness. With this in mind, we shall proceed using σ since it results in shorter expressions.
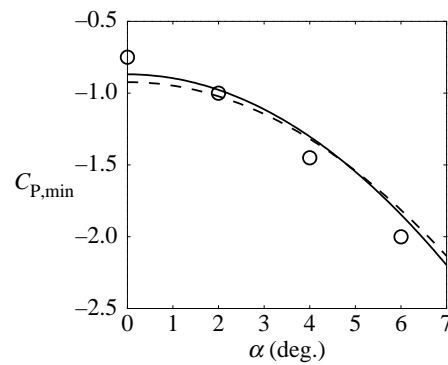
Figure 7. Minimal pressure coefficient on the surface of a 0.2 chord thick dolphin caudal fin. Circles mark the data extracted from fig. 2 of Lang (1966), dashed line marks the approximation (A 12) with $t = 0.2c$ and solid line marks the approximation (A 14) with $r_{\mathrm{LE}} = 0.042c$.

Cavitation first appears when the lowest pressure on the aerofoil drops below the vapour pressure, p_{v}. Since the former decreases with the angle of attack, see equation (A 12), cavitation will be avoided if the angle of attack is kept below

$$\alpha_{\mathrm{c}} = \sigma\sqrt{\frac{K - 6\sigma}{1 + 6\sigma}} + O(\varepsilon^2)$$
$$= \sigma\sqrt{K - 6\sigma} + O(\varepsilon^2), \qquad (A\ 15)$$

the angle of attack where the lowest pressure on the aerofoil $p_{\min}$ equals p_{v}. Here,

$$K = 2\frac{p_{\mathrm{d}} - p_{\mathrm{v}}}{\rho u_\infty^2} \qquad (A\ 16)$$

is the cavitation number (Batchelor 1990). Since the lift coefficient of a Joukowski aerofoil is

$$C_{\mathrm{L}} = 2\pi(1 + \sigma)\alpha + O(\varepsilon^3) = 2\pi\alpha + O(\varepsilon^2) \qquad (A\ 17)$$

(Batchelor 1990). Equation (A 15) implies that cavitation will first develop when the section lift coefficient will reach

$$C_{\mathrm{L,c}} = 2\pi\sigma\sqrt{K - 6\sigma} + O(\varepsilon^2). \qquad (A\ 18)$$

The pressure of the unperturbed fluid, p_{d}, changes with depth d by

$$p_{\mathrm{d}} + p_0 = \rho g d, \qquad (A\ 19)$$

where p_0 is the atmospheric pressure and g is the acceleration owing to gravity. Moreover, at relevant water temperatures, p_{v} measures one hundredth of an atmosphere and hence can be practically neglected. Accordingly, equation (A 18) can be recast as

$$C_{\mathrm{L,c}} \approx 2\pi\sigma\sqrt{\frac{2(p_0 + \rho g d)}{\rho u_\infty^2} - 6\sigma} \qquad (A\ 20)$$

or, equivalently,

$$C_{\mathrm{L,c}} \approx \tau\sqrt{\frac{u_{\mathrm{d}}^2 - u_\infty^2}{u_\infty^2}}, \qquad (A\ 21)$$

where

$$\tau = \pi\sqrt{24\sigma^3} = \pi\sqrt[4]{\frac{72 r_{\mathrm{LE}}^3}{c^3}}, \qquad (A\ 22)$$

is a shape parameter and

$$u_{\mathrm{d}} = \sqrt{\frac{p_0 + \rho g d}{3 \sigma \rho}} = \sqrt[4]{\frac{2c}{9 r_{\mathrm{LE}}}} \sqrt{\frac{p_0 + \rho g d}{\rho}} \qquad \text{(A 23)}$$

is a cavitation velocity constant. It can be loosely interpreted as a velocity at which cavitation appears with no lift (see the text following equation (A13)). Noting that $u_\infty^2 = u^2 + v^2 = u^2(1 + \bar{v}^2)$, equation (2.11) immediately follows.

APPENDIX B. MINIMAL POWER

Given the lift and drag coefficients of the caudal fin, C_{L} and $C_{\mathrm{D}} = C_{\mathrm{D},0} + kC_{\mathrm{L}}^2$, as well as the drag coefficient of the fish body, $C_{\mathrm{D,b}}$, sustained swimming with constant forward velocity u is possible only if the tail moves with lateral velocity $v = u\bar{v}$, where $\bar{v}$ is the solution of

$$(C_{\mathrm{L}}\bar{v} - C_{\mathrm{D}})\sqrt{1 + \bar{v}^2} = C_{\mathrm{D,b}} \qquad \text{(B 1)}$$

(see equation (2.5)). The associated propulsion efficiency is given by

$$\eta = \frac{C_{\mathrm{D,b}}}{C_{\mathrm{D,b}} + (1 + \bar{v}^2)^{3/2} C_{\mathrm{D}}} \qquad \text{(B 2)}$$

(see equation (2.9)). We seek the lift coefficient C_{L}^+ and the associated $\bar{v}^+$ yielding minimum for η.

First, let us assume that η has an extremum at $C_{\mathrm{L}} = C_{\mathrm{L}}^+$. In this event, the derivative $\mathrm{d}\eta/\mathrm{d}C_{\mathrm{L}}$ vanishes, and therefore

$$\frac{\partial \bar{v}}{\partial C_{\mathrm{L}}} \frac{3\bar{v}}{1 + \bar{v}^2} + \frac{2kC_{\mathrm{L}}}{C_{\mathrm{D}}} \quad \text{at } C_{\mathrm{L}} = C_{\mathrm{L}}^+. \qquad \text{(B 3)}$$

But

$$\frac{\bar{v} + C_{\mathrm{L}}\frac{\partial \bar{v}}{\partial C_{\mathrm{L}}} - 2kC_{\mathrm{L}}}{(C_{\mathrm{L}}\bar{v} - C_{\mathrm{D}})} + \frac{\bar{v}\frac{\partial \bar{v}}{\partial C_{\mathrm{L}}}}{1 + \bar{v}^2} = 0, \qquad \text{(B 4)}$$

by equation (B 1). Hence, upon eliminating $\partial \bar{v}/\partial C_{\mathrm{L}}$, one finds

$$3C_{\mathrm{D},0}\bar{v}^2 - kC_{\mathrm{L}}\big(4C_{\mathrm{D},0}\bar{v} + 4k\bar{v}C_{\mathrm{L}}^2 + C_{\mathrm{L}}(2 + \bar{v}^2)\big) = 0$$

$$\text{at } C_{\mathrm{L}} = C_{\mathrm{L}}^+. \qquad \text{(B 5)}$$

Setting, temporarily,

$$\bar{v} = wC_{\mathrm{L}}, \qquad \text{(B 6)}$$

where w is a certain function of C_{L}, one arrives at

$$C_{\mathrm{L}}^2 = \frac{3C_{\mathrm{D},0}w^2 - 4kC_{\mathrm{D},0}w - 2k}{4k^2 w + w^2 k} \quad \text{at } C_{\mathrm{L}} = C_{\mathrm{L}}^+ \quad \text{(B 7)}$$

and, obviously,

$$\bar{v} = w\sqrt{\frac{3C_{\mathrm{D},0}w^2 - 4kC_{\mathrm{D},0}w - 2k}{4k^2 w + w^2 k}} \quad \text{at } C_{\mathrm{L}} = C_{\mathrm{L}}^+. \quad \text{(B 8)}$$

Substituting equations (B 7) and (B 8) into equation (B 2) yields a single equation for w, which can be easily solved numerically. An approximate analytical solution follows.

It is well known that $C_{\mathrm{L}}^* = \sqrt{C_{\mathrm{D},0}/k}$ is the lift coefficient yielding maximal lift-to-drag ratio $E^* = (2\sqrt{C_{\mathrm{D},0}k})^{-1}$ of the aerodynamic surface—a fin, in our case. With these, let $\bar{C}_{\mathrm{L}} = C_{\mathrm{L}}/C_{\mathrm{L}}^*$ and $\bar{C}_{\mathrm{D,b}} = C_{\mathrm{D,b}}/C_{\mathrm{L}}^*$; consequently, equation (B 5) can be

rewritten as

$$3\bar{v}^2 - \frac{2\bar{v}\bar{C}_{\mathrm{L}}}{E^*}\big(1 + \bar{C}_{\mathrm{L}}^2\big) - \bar{C}_{\mathrm{L}}^2(2 + \bar{v}^2) = 0 \quad \text{at } C_{\mathrm{L}} = C_{\mathrm{L}}^+.$$

$$\text{(B 9)}$$

But E^* is typically very large (a few tens), whereas C_{L}^* is of the order of unity. Thus assuming, subject of course to an *a posteriori* verification, that $\bar{v}$ and $\bar{C}_{\mathrm{L}}$ are each of the order of unity as well, the term involving E^* in equation (B 9) can be neglected, leaving

$$\bar{v}^2 \approx \frac{2\bar{C}_{\mathrm{L}}^2}{3 - \bar{C}_{\mathrm{L}}^2} \quad \text{at } C_{\mathrm{L}} = C_{\mathrm{L}}^+. \qquad \text{(B 10)}$$

Substituting it back into equation (B 1) yields an equation for the optimal lift coefficient

$$\left(\bar{C}_{\mathrm{L}}^+ \sqrt{\frac{2\bar{C}_{\mathrm{L}}^{+2}}{3 - \bar{C}_{\mathrm{L}}^{+2}}} - \frac{1}{2E^*}\big(1 + \bar{C}_{\mathrm{L}}^{+2}\big)\right) \sqrt{1 + \frac{2\bar{C}_{\mathrm{L}}^{+2}}{3 - \bar{C}_{\mathrm{L}}^{+2}}} = \bar{C}_{\mathrm{D,b}}.$$

$$\text{(B 11)}$$

Equation (B 11) can be simplified further by neglecting the term involving E^* (using the same arguments as in equation (B 10)). The result is

$$\frac{\bar{C}_{\mathrm{L}}^{+2}}{3 - \bar{C}_{\mathrm{L}}^{+2}} \sqrt{2\big(3 + \bar{C}_{\mathrm{L}}^{+2}\big)} = \bar{C}_{\mathrm{D,b}}. \qquad \text{(B 12)}$$

This equation possesses an analytical solution for $\bar{C}_{\mathrm{L}}^+$ (it reduces to a third-order equation), but it is too lengthy to be presented here explicitly. Substituting equations (B 12) and (B 10) back into equation (B 1) yields the minimal efficiency

$$E^*\left(\frac{1 - \eta^+}{\eta^+}\right) \approx \left(\frac{3 + \bar{C}_{\mathrm{L}}^{+2}}{3 - \bar{C}_{\mathrm{L}}^{+2}}\right)^{3/2} \frac{1 + \bar{C}_{\mathrm{L}}^{+2}}{2\bar{C}_{\mathrm{D,b}}}. \qquad \text{(B 13)}$$

Since $\bar{C}_{\mathrm{L}}^+$ is a function of $\bar{C}_{\mathrm{D,b}}$ only by equation (B 12), it immediately follows that the right-hand side of equation (B 13) is a function of $\bar{C}_{\mathrm{D,b}}$ only as well. This result is the basis of the graphical representation in figure 2.

APPENDIX C. MINIMAL LATERAL TAIL VELOCITY

Given the lift and drag coefficients of the caudal fin, C_{L} and $C_D = C_{D,0} + kC_L^2$, as well as the drag coefficient of the fish body, $C_{\mathrm{D,b}}$, sustained swimming with constant forward velocity u is possible only if the tail moves with lateral velocity $v = u\bar{v}$, where $\bar{v}$ is the solution of

$$(C_{\mathrm{L}}\bar{v} - C_{\mathrm{D}})\sqrt{1 + \bar{v}^2} = C_{\mathrm{D,b}} \qquad \text{(C 1)}$$

(equation (2.5)). We seek the lift coefficient C_{L}^* yielding minimum for $\bar{v}$, or, in other words, we seek the lift coefficient of the tail for which swimming with velocity u requires the slowest tail motion.

First, let us assume that $\bar{v}$ has an extremum at $C_{\mathrm{L}} = C_{\mathrm{L}}^*$. In this event, the derivative $\mathrm{d}\bar{v}/\mathrm{d}C_{\mathrm{L}}$ vanishes, and therefore by differentiating on both sides of equation (C1) with respect to C_{L} we readily obtain

$$\bar{v} - 2kC_L = 0 \quad \text{at } C_{\mathrm{L}} = C_{\mathrm{L}}^*; \qquad \text{(C 2)}$$

C_L^* is the solution of the conjunction of equations (C1) and (C2).

For high aspect ratio fins, k is of the order of 0.1.[2] Assuming, subject to a *posteriori* verification, that C_L^* is of the order of unity, equation (C2) implies that $\bar{v}$ at $C_L = C_L^*$ is of the order of k and, hence, small as compared with unity. Consequently, the conjunction of equations (C1) and (C2) yields

$$\left(2kC_L^{*2} - C_{D,0}\right)\left(1 + 2k^2 C_L^{*2} + \cdots\right) = C_{D,b}, \qquad \text{(C 3)}$$

where the ellipsis stands for higher order terms with respect to k. Its leading order solution is

$$C_L^* \approx \sqrt{\frac{(C_{D,0} + C_{D,b})}{k}}. \qquad \text{(C 4)}$$

With the typical $C_{D,0} \sim 0.01$, $C_{D,b} \sim 0.2$ and $k \sim 0.1$, it immediately follows that this optimal lift coefficient equals approximately 1.5. It is, indeed, of the order of unity, but greater than the maximal attainable lift coefficient $C_{L,max}$. Hence, $\bar{v}$ has no extremum for admissible values of the lift coefficients, and it attains a minimum at the maximal lift coefficient possible, i.e. at $C_{L,max}$.

REFERENCES

Azuma, A. 1992 The biokinetics of flying and swimming, p. 16. Tokyo, Japan: Springer.

Batchelor, G. K. 1990 Introduction to fluid dynamics. Cambridge University Press Cambridge, UK.

Cheng, H. K. & Murillo, L. E. 1984 Lunate-tail swimming propulsion as a problem of curved lifting line in unsteady flow. Part 1. Asymptotic theory. *J. Fluid Mech.* **143**, 327–350. (doi:10.1017/S0022112084001373)

Chopra, M. G. 1974 Hydromechanics of lunate-tail swimming propulsion. *J. Fluid Mech.* **64**, 375–391. (doi:10.1017/S002211207400245X)

Chopra, M. G. 1976 Large amplitude lunate-tail theory of fish locomotion. *J. Fluid Mech.* **74**, 161–182. (doi:10.1017/S0022112076001742)

Chopra, M. G. & Kambe, T. 1977 Hydromechanics of lunate-tail swimming propulsion. Part 2. *J. Fluid Mech.* **79**, 49–69. (doi:10.1017/S0022112077000032)

Collinsworth, A. M., Zhang, S., Kraus, W. E. & Truskey, G. A. 2002 Apparent elastic modulus and hysteresis of skeletal muscle cells throughout differentiation. *Am. J. Phys. Cell Physiol.* **283**, C1219–C1227.

Fish, F. E. & Rohr, J. J. 1999 Review of dolphin hydrodynamics and swimming performance. SPAWAR Technical Report no. 1081.

Graff, K. F. 1975 Wave motion in elastic solids, p. 77. Oxford, UK: Clarendon Press.

Gray, J. 1936 Studies in animal locomotion. VI. The propulsive powers of the dolphin. *J. Exp. Biol.* **13**, 192–199.

Jacobs, E. N. 1931a Aerodynamic characteristics of eight very thick airfoils from tests in the variable density tunnel. NACA Report no. 378.

Jacobs, E. N. 1931b Tests of six symmetrical airfoils in the variable density tunnel. NACA Report no. 385.

Johnston, I. 1983 Dynamic properties of fish muscle. In *Fish biomechanics* (eds D. Webb & D. Weihs), pp. 36–67. New York, NY: Praeger.

Katz, J. & Weihs, D. 1978 Hydrodynamic propulsion by large amplitude oscillation of an airfoil with chordwise flexibility. *J. Fluid Mech.* **88**, 485–498. (doi:10.1017/S0022112078002220)

Kishinouye, K. 1923 Contributions to the comparative studies of the so-called scombroid fishes. *J. Coll. Agric. Imperial Univ. Tokyo* **8**, 293–475.

Lang, T. G. 1966 Hydrodynamic analysis of dolphin fin profiles. *Nature* **209**, 1110–1111. (doi:10.1038/2091110a0)

Lighthill, M. J. 1969 Hydromechanics of aquatic animal propulsion. *Annu. Rev. Fluid Mech.* **1**, 413–447. (doi:10.1146/annurev.fl.01.010169.002213)

Lighthill, M. J. 1970 Aquatic animal propulsion of high hydromechanical efficiency. *J. Fluid Mech.* **44**, 265–301. (doi:10.1017/S0022112070001830)

Lingham-Soliar, T. 2005 Caudal fin in the white shark. *Carcharodon Carcharias* (lamnidae): a dynamic propeller for fast, efficient swimming. *J. Morphol.* **264**, 233–252. (doi:10.1002/jmor.10328)

Magnuson, J. J. 1978 Locomotion by scombrid fishes: hydromechanics, morphology and behavior. In *Fish physiology*, vol. VII (eds W. S. Hoar & D. J. Randall), pp. 239–313. New York, NY: Academic Press.

Milne-Thomson, L. M. 1973 Theoretical aerodynamics, pp. 97–99, 4th edn. New York, NY: Dover.

Nicolai, L. M. 1984 Fundamentals of aircraft design, pp. 11.8–11.11. San Jose, CA: METS, Inc.

Vander, A. J., Sherman, J. H. & Luciano, D. S. 1985 Human physiology, pp. 255–298, 4th edn. New York, NY: McGraw Hill.

Walters, V. & Fierstein, H. L. 1964 Measurements of swimming speeds of yellowfin tuna and wahoo. *Nature* **202**, 208–209. (doi:10.1038/202208b0)

Wardle, C. S. 1975 Limit of fish swimming speed. *Nature* **255**, 725–727. (doi:10.1038/255725a0)

Wardle, C. S. & Videler, J. J. 1980 How do fish break the speed limit? *Nature* **284**, 445–447. (doi:10.1038/284445a0)

Weihs, D. 2004 The hydrodynamics of dolphin drafting. *J. Biol.* **3**, 1–16. (doi:10.1186/jbiol2)